

# **Supporting information for:**

## **Performance of Van der Waals Corrected Functionals for Guest Adsorption in the M<sub>2</sub>(dobdc) Metal–Organic Frameworks**

Bess Vlaisavljevich,<sup>1</sup> Johanna Huck,<sup>1</sup> Zeric Hulvey,<sup>2,3</sup> Kyuho Lee,<sup>4</sup> Jarad A. Mason,<sup>5</sup> Jeffrey Neaton,<sup>4</sup> Jeffrey R. Long,<sup>5,6</sup> Craig M. Brown<sup>2,7</sup> Dario Alfe,<sup>8</sup> Angelos Michaelides,<sup>9</sup> and Berend Smit<sup>1,10,\*\*</sup>

<sup>1</sup>*Department of Chemical and Biomolecular Engineering, University of California, Berkeley, California, 94720, USA,* <sup>2</sup>*Center for Neutron Research, National Institute of Standards and Technology, Gaithersburg, Maryland, 20899, USA,* <sup>3</sup>*Department of Materials Science and Engineering, University of Maryland, College Park, Maryland, 20742, USA,* <sup>4</sup>*Molecular Foundry, Lawrence Berkeley National Laboratory, Berkeley, California, 94720, USA,*  
<sup>5</sup>*Department of Chemistry, University of California, Berkeley, California, 94720, USA,* <sup>6</sup>*Materials Science Division, Lawrence Berkeley National Laboratory, Berkeley, California, 94720, USA,* <sup>7</sup>*Department of Chemical and Biomolecular Engineering, University of Delaware, Newark, Delaware, 19716, USA,* <sup>8</sup>*Department of Earth Sciences, Thomas Young Centre and London Centre for Nanotechnology, University College London, Gower Street, London WC1E 6BT, United Kingdom,* <sup>9</sup>*Thomas Young Centre, London Centre for Nanotechnology and Department of Physics and Astronomy, University College London, 25 Gower Street, London WC1E 6BT, United Kingdom,* <sup>10</sup>*Institut des Sciences et Ingénierie Chimiques, Valais, Ecole Polytechnique Fédérale de Lausanne (EPFL), Rue de l'Industrie 17, CH-1951 Sion, Switzerland,*  
<sup>11</sup>*Department of Physics, University of California, Berkeley, California, 94720, USA,* <sup>12</sup>*Kavli Energy Nanosciences Institute at Berkeley, Berkeley, California, 94720, USA*

E-mail: berend-smit@berkeley.edu

# 1 Values for plotted data in the main article

## 1.1 Geometric Parameters for the Optimized Framework

Table S1: Calculated and experimental lattice constants and metal-oxygen distances for  $M_2(\text{dobdc})$  where  $M = \text{Mg}, \text{Mn}, \text{Fe}, \text{Co}, \text{Ni}, \text{Cu}, \text{or Zn}$ . The basal M-O bond distances are the average of all four basal M-O bonds. These values are plotted in Figure 2.

Metal	method	Lattice Constants ( $\text{\AA}$ )		M-O Distance ( $\text{\AA}$ )	
		a+b	c	apical	basal
Mg	ND at 10K	25.92	6.86	2.08	2.01
	PBE	26.07	6.93	2.02	2.04
	opt88B-vdW	26.03	6.91	2.03	2.04
	opt86b-vdW	26.01	6.90	2.02	2.03
	vdW-DF2	26.21	6.95	2.04	2.05
	rev-vdW-DF2	26.01	6.91	2.02	2.03
	PBE-D2	26.01	6.88	2.01	2.03
	PBE-D3	26.04	6.92	2.02	2.04
	PBE-D3 BJ	26.03	6.91	2.02	2.04
	M06-L	25.78	6.83	1.99	2.01
	XRD	26.23	7.04	2.21	2.10
	PBE	26.55	7.16	2.16	2.14
Mn	opt88B-vdW	26.47	7.11	2.16	2.13
	opt86b-vdW	26.44	7.09	2.15	2.12
	vdW-DF2	26.72	7.20	2.20	2.16
	rev-vdW-DF2	26.44	7.10	2.15	2.12
	PBE-D2	26.47	7.14	2.16	2.13
	PBE-D3	26.51	7.15	2.16	2.14
	PBE-D3 BJ	26.48	7.14	2.15	2.13
	ND at 9K	26.10	6.85	2.13	2.09
	PBE	26.47	6.97	2.13	2.08
	opt88B-vdW	26.39	6.91	2.12	2.07
	opt86b-vdW	26.36	6.89	2.11	2.06
	vdW-DF2	26.65	7.01	2.17	2.10
Fe	rev-vdW-DF2	26.36	6.90	2.11	2.06
	PBE-D2	26.40	6.94	2.13	2.07
	PBE-D3	26.44	6.96	2.13	2.08
	PBE-D3 BJ	26.42	6.95	2.12	2.07
	XRD at 368K	25.89	6.81	2.07	2.02
	PBE	26.20	6.91	2.09	2.05
	opt88B-vdW	26.06	6.81	2.07	2.03
	opt86b-vdW	26.02	6.80	2.06	2.02
	vdW-DF2	26.33	6.91	2.13	2.07
	rev-vdW-DF2	26.06	6.85	2.04	2.03
	PBE-D2	26.07	6.84	2.08	2.04
	PBE-D3	26.10	6.84	2.08	2.04
Co	PBE-D3 BJ	26.08	6.83	2.07	2.03
	XRD at 295 K	25.79	6.77	2.07	1.99
	PBE	25.97	6.84	2.06	2.03
	opt88B-vdW	25.79	6.72	2.04	2.00
	opt86b-vdW	25.74	6.71	2.02	1.99
	vdW-DF2	26.10	6.87	2.07	2.04
	rev-vdW-DF2	25.73	6.72	2.02	1.99
	PBE-D2	25.82	6.75	2.04	2.00
	PBE-D3	25.83	6.75	2.04	2.00
	PBE-D3 BJ	25.80	6.74	2.04	2.00
	XRD at 100 K	26.00	6.26	2.50	1.97
	PBE	26.16	6.36	2.44	1.98
Ni	optB88-vdW	26.06	6.19	2.48	1.96
	optB86b-vdW	26.00	6.18	2.45	1.96
	vdW-DF2	26.43	6.37	2.55	2.01
	rev-vdW-DF2	25.99	6.20	2.45	1.96
	PBE-D2	26.09	6.28	2.49	1.97
	PBE-D3	26.12	6.30	2.46	1.97
	PBE-D3 BJ	26.08	6.28	2.44	1.97
	ND at 10K	25.89	6.82	2.08	2.05
	PBE	26.09	7.00	2.03	2.08
	opt88B-vdW	26.00	6.95	2.03	2.07
	opt86b-vdW	25.98	6.93	2.03	2.06
	vdW-DF2	26.26	7.05	2.08	2.10
Cu	rev-vdW-DF2	25.98	6.94	2.03	2.13
	PBE-D2	26.02	6.97	2.04	2.07
	PBE-D3	26.05	6.98	2.03	2.08
	PBE-D3 BJ	26.04	6.97	2.03	2.07
	M06-L	25.80	6.61	2.08	2.03

## 1.2 Guest Electronic Binding Energies

Table S2: Methane binding in  $M_2(\text{dobdc})$  with four vdW corrected functionals using the rigid framework approximation. Geometries were optimized with a 550 eV cutoff and single points were performed with a 1000 eV cut off to compute the binding energies. The geometries and binding energies of PBE-D3 and PBE-D3 BJ were optimized with a 1000 eV cut off. Values plotted in Figure 4

Metal	optB88-vdW	optB86b-vdW	vdW-DF2	rev-vdW-DF2	PBE-D2	PBE-D3	PBE-D3 BJ	M06-L	Exp.	Corrected Exp.
Mg	-33.1	-33.7	-25.9	-26.1	-31.3	-29.3	-26.4	-27.6	-19.0	-23.8
Mn	-32.4	-33	-24.6	-25.5	-28.8	-28.8	-26.1	-19.0	-23.0	
Fe	-31.7	-32	-24.4	-24.5	-28.3	-28.5	-24.9	-20.0	-20.0	-24.4
Co	-28.6	-31.9	-24.1	-21.5	-24.9	-24.1	-20.9	-20.0	-20.0	-24.4
Ni	-31.6	-31.9	-24.7	-24.5	-28	-27	-23.7	-20.0	-20.0	-24.3
Cu	-24.9	-24.8	-19.3	-17.7	-20.2	-21.4	-18.6	-14.0	-14.0	-18.4
Zn	-31.3	-31.7	-23.8	-24.1	-27.6	-27.7	-24.3	-26.5	-18.0	-22.6

Table S3:  $\text{CO}_2$  binding in  $M_2(\text{dobdc})$  with four vdW corrected functionals using the rigid framework approximation. Geometries were optimized with a 550 eV cutoff and single points were performed with a 1000 eV cut off to compute the binding energies. The geometries and binding energies of PBE-D3 and PBE-D3 BJ were optimized with a 1000 eV cut off. Values plotted in Figure 4

Metal	optB88-vdW	optB86b-vdW	vdW-DF2	rev-vdW-DF2	PBE-D2	PBE-D3	PBE-D3 BJ	M06-L	Exp.	Corrected Exp.
Mg	-53.1	-52.5	-45.2	-43.6	-40.5	-39.7	-40.5	-42.8	-43.5	-47.2
Mn	-46.2	-45.9	-38.1	-37.0	-33.8	-34.6	-35.5	-31.7	-31.7	-35.3
Fe	-46.5	-46.1	-38.1	-37.3	-33.9	-34.5	-35.3	-33.2	-33.2	-36.8
Co	-46.7	-46.6	-37.7	-37.4	-33.7	-33.9	-34.5	-33.6	-33.6	-37.2
Ni	-51.0	-50.7	-41.5	-41.3	-36.9	-36.7	-37.4	-38.6	-38.6	-42.3
Cu	-37.9	-37.5	-30.9	-28.2	-27.1	-28.0	-27.8	-22.1	-22.1	-25.7
Zn	-41.6	-41.3	-34.0	-32.1	-30.5	-31.8	-31.0	-32.5	-26.8	-30.4

Table S4: Water binding in  $M_2(\text{dobdc})$  with four vdW corrected functionals. Atomic positions and lattice constants were optimized for framework and guest atoms. Geometries were optimized with a 550 eV cutoff and single points were performed with a 1000 eV cut off to compute the binding energies. The geometries and binding energies of PBE-D3 and PBE-D3 BJ were optimized with a 1000 eV cut off. Values plotted in Figure 4

Metal	optB88-vdW	optB86b-vdW	vdW-DF2	rev-vdW-DF2	PBE-D2	PBE-D3	PBE-D3 BJ	M06-L
Mg	-86.0	-85.9	-77.8	-81.2	-81.6	-81.1	-79.6	-84.2
Mn	-70.5	-70.8	-63.4	-65.5	-68.4	-66.5	-66.9	
Fe	-71.7	-71.9	-63.5	-67.2	-68.7	-68.9	-66.9	
Co	-70.1	-70.5	-63.4	-64.3	-68.0	-65.7	-63.6	
Ni	-83.6	-83.9	-73.7	-78.4	-79.7	-78.1	-75.9	
Cu	-44.0	-44.1	-37.9	-38.9	-34.2	-36.4	-39.5	
Zn	-64.8	-65.5	-55.3	-60.5	-61.5	-62.5	-60.2	-63.6

### 1.3 Guest Binding Geometries

Table S5: M-C distances in Å for methane binding in  $M_2(\text{dobdc})$  with eight vdW corrected functionals using the rigid framework approximation. Geometries were optimized with a 550 eV cutoff for all cases except for PBE-D3 and PBE-D3 BJ where optimizations were performed with a 1000 eV cut off. Experiments performed with  $\text{CD}_4$ . Values plotted in Figure 5

Metal	optB88-vdW	optB86b-vdW	vdW-DF2	rev-vdW-DF2	PBE-D2	PBE-D3	PBE-D3 BJ	M06-L	Exp.
Mg	2.954	2.978	3.106	2.954	2.859	3.108	3.108	2.947	2.952
Mn	2.956	2.955	3.148	2.956	2.956	2.956	2.955		2.933
Fe	2.988	2.951	3.184	2.944	2.952	3.017	2.953		2.903
Co	3.003	2.978	3.197	2.985	2.979	2.981	2.979		2.953
Ni	3.046	3.030	3.198	3.061	2.992	3.031	3.030		2.951
Cu	3.426	3.426	3.427	3.426	3.256	3.426	3.427		3.281
Zn	3.075	3.062	3.246	3.057	3.061	3.063	3.062	2.999	3.091

Table S6: M-O distances in Å for  $\text{CO}_2$  binding in  $M_2(\text{dobdc})$  with eight vdW corrected functionals using the rigid framework approximation. Geometries were optimized with a 550 eV cutoff for all cases except for PBE-D3 and PBE-D3 BJ where optimizations were performed with a 1000 eV cut off. Values plotted in Figure 5

Metal	optB88-vdW	optB86b-vdW	vdW-DF2	rev-vdW-DF2	PBE-D2	PBE-D3	PBE-D3 BJ	M06-L	Exp.
Mg	2.338	2.349	2.410	2.358	2.369	2.411	2.410	2.342	2.270
Mn	2.499	2.501	2.574	2.506	2.537	2.559	2.544		2.510
Fe	2.472	2.466	2.616	2.471	2.536	2.576	2.557		2.290
Co	2.454	2.432	2.563	2.461	2.514	2.563	2.524		2.230 / 2.262
Ni	2.387	2.373	2.539	2.384	2.450	2.521	2.473		2.290
Cu	2.780	2.787	2.872	2.840	2.897	2.873	2.873		2.860
Zn	2.698	2.717	2.837	2.746	2.836	2.837	2.789	2.551	2.430

Table S7: M-O distances in Å for  $\text{H}_2\text{O}$  binding in  $M_2(\text{dobdc})$  with eight vdW corrected functionals. Geometries were optimized with a 550 eV cutoff for all cases except for PBE-D3 and PBE-D3 BJ where optimizations were performed with a 1000 eV cut off. Values plotted in Figure 5

Metal	optB88-vdW	optB86b-vdW	vdW-DF2	rev-vdW-DF2	PBE-D2	PBE-D3	PBE-D3 BJ	M06-L	Exp.
Mg	2.136	2.136	2.162	2.134	2.127	2.135	2.209	2.105	
Mn	2.280	2.280	2.323	2.280	2.287	2.293	2.340		
Fe	2.234	2.230	2.285	2.229	2.238	2.241	2.300		
Co	2.203	2.198	2.257	2.205	2.209	2.215	2.261		2.137(0)
Ni	2.121	2.117	2.188	2.119	2.129	2.135	2.193		
Cu	2.357	2.360	2.417	2.360	2.417	2.389	2.595		
Zn	2.221	2.211	2.288	2.217	2.219	2.224	2.316	2.214	

## 2 Additional Geometric Parameters

Table S8: M-O-C bonding angle in degrees for CO<sub>2</sub> binding in M<sub>2</sub>(dobdc) with eight vdW corrected functionals using the rigid framework approximation. Geometries were optimized with a 550 eV cutoff for all cases except for PBE-D3 and PBE-D3 BJ where optimizations were performed with a 1000 eV cut off.

Metal	optB88-vdW	optB86b-vdW	vdW-DF2	rev-vdW-DF2	PBE-D2	PBE-D3	PBE-D3 BJ	M06-L	Exp.
Mg	123.7	124.0	123.8	125.6	123.3	123.8	123.8	125.0	131.0
Mn	122.5	122.5	122.1	123.6	121.1	123.2	123.4		120.0
Fe	121.0	121.9	120.6	121.0	119.6	122.0	122.2		106.0
Co	120.6	119.9	118.6	119.6	119.4	118.6	119.9		118.0
Ni	120.5	120.6	119.2	121.8	120.8	120.3	121.2		117.0
Cu	114.0	114.1	112.4	113.1	109.9	112.4	112.4		117.0
Zn	117.0	116.2	114.6	117.2	114.5	114.7	116.3	118.0	117.0

Table S9: M-O distances in Å for H<sub>2</sub>O binding in M<sub>2</sub>(dobdc) with eight vdW corrected functionals using the rigid framework approximation. Geometries were optimized with a 550 eV cutoff for all cases except for PBE-D3 and PBE-D3 BJ where optimizations were performed with a 1000 eV cut off.

Metal	optB88-vdW	optB86b-vdW	vdW-DF2	rev-vdW-DF2	PBE-D2	PBE-D3	PBE-D3 BJ	M06-L	Exp.
Mg	2.205	2.201	2.259	2.201	2.190	2.215	2.209	2.159	
Mn	2.323	2.315	2.395	2.321	2.333	2.343	2.340		
Fe	2.291	2.274	2.377	2.270	2.289	2.303	2.300		
Co	2.251	2.238	2.347	2.235	2.257	2.267	2.261		2.137(0)
Ni	2.188	2.169	2.289	2.170	2.189	2.203	2.193		
Cu	2.553	2.545	2.693	2.546	2.552	2.572	2.595		
Zn	2.311	2.291	2.450	2.295	2.303	2.326	2.316	2.264	

## 3 Convergence Tests

### 3.1 Rigid Framework Approximation

Table S10: The validity of the rigid framework approximation was tested by performing full geometry optimizations with the optB88-vdW functional using a 1000 eV cut off for CO<sub>2</sub> and CH<sub>4</sub> in the Mg<sub>2</sub>(dobdc) framework. Binding energies in kJ/mol.

Guest	Binding Energy (Full Optimization)	Binding Energy (Rigid FW)
CO <sub>2</sub>	-56.0	-53.6
CH <sub>4</sub>	-34.2	-33.1

Table S11: Water binding in  $M_2(\text{dobdc})$  using the rigid framework approximation. Geometries were optimized using a cutoff of 550 eV and single point calculations were performed using a 1000 eV cut-off. The geometries and binding energies of PBE-D3 and PBE-D3 BJ were optimized with a 1000 eV cut off. Energies are in kJ/mol. The rigid framework approximation is not valid for water. Comparisons with Table S9 can be made.

Metal	optB88-vdW	optB86b-vdW	vdW-DF2	rev-vdW-DF2	PBE-D2	PBE-D3	PBE-D3 BJ	M06-L
Mg	-76.7	-76.8	-67.3	-71.9	-72.3	-71.4	-69.9	-75.2
Mn	-66.1	-66.6	-56.1	-61.8	-61.4	-61.0	-59.5	
Fe	-66.0	-66.8	-54.5	-62.1	-61.3	-51.7	-59.9	
Co	-65.8	-66.9	-53.2	-61.8	-61.1	-60.7	-59.0	
Ni	-75.6	-76.8	-61.5	-71.7	-70.1	-69.3	-67.5	
Cu	-35.4	-35.9	-28.0	-30.9	-30.8	-32.7	-30.4	
Zn	-58.7	-59.7	-46.6	-54.4	-54.2	-55.2	-52.9	-59.1

Table S12: The effect of the plane wave energy cut off and the  $\Gamma$  approximation on the optimized geometries (lattice parameters in Å) of the frameworks was tested for the  $M_2(\text{dobdc})$ . Plane wave cutoffs and K-point sampling are noted. A 2x2x2 Monkhorst grid was applied only for the Mg framework. The opt88B-vdW functional was used.

Level of theory	Metal	a=b	c
$\Gamma$ / 550 eV	Mg	26.03	6.91
$\Gamma$ / 1000 eV	Mg	26.04	6.90
2x2x2 / 1000 eV	Mg	26.07	6.93
$\Gamma$ / 550 eV	Mn	26.47	7.11
$\Gamma$ / 1000 eV	Mn	26.47	7.11
$\Gamma$ / 550 eV	Fe	26.03	6.91
$\Gamma$ / 1000 eV	Fe	26.04	6.90
$\Gamma$ / 550 eV	Co	26.06	6.81
$\Gamma$ / 1000 eV	Co	26.06	6.81
$\Gamma$ / 550 eV	Ni	25.79	6.72
$\Gamma$ / 1000 eV	Ni	25.79	6.72
$\Gamma$ / 550 eV	Cu	26.04	6.18
$\Gamma$ / 1000 eV	Cu	26.06	6.19
$\Gamma$ / 550 eV	Zn	26.01	6.95
$\Gamma$ / 1000 eV	Zn	26.00	6.95

Table S13: The effect of the plane wave energy cut off and the  $\Gamma$  approximation on the binding energies (in kJ/mol) was tested for the  $Mg_2(\text{dobdc})$ . Plane wave cutoffs and K-point sampling are noted. The opt88B-vdW functional was used. A 2x2x2 or 4x4x4 Monkhorst grid was applied when noted.

Guest	$\Gamma$ / 550 eV	$\Gamma$ / 1000 eV	2x2x2 / 550 eV	2x2x2 / 1000 eV	4x4x4 / 550 eV	4x4x4 / 1000 eV
$\text{CO}_2$	-53.1	-53.1	-53.3	-53.4	-53.3	-53.4

Table S14: The effect of the plane wave energy cut off on the CO<sub>2</sub> binding energies (in kJ/mol) was tested for all of the M<sub>2</sub>(dobdc) with the opt88B-vdW functional.

Metal	550 eV	SP with 1000 eV	1000 eV
Mg	-53.1	-53.1	-53.6
Mn	-46.1	-46.2	-46.1
Fe	-46.4	-46.5	-46.3
Co	-46.7	-46.7	-46.5
Ni	-50.9	-51.0	-51.0
Cu	-38.1	-37.9	-38.0
Zn	-41.5	-41.6	-41.6

Table S15: The effect of the plane wave energy cut off on the CH<sub>4</sub> binding energies (in kJ/mol) was tested for all of the M<sub>2</sub>(dobdc) with the opt88B-vdW functional.

Metal	550 eV	SP with 1000 eV	1000 eV
Mg	-33.1	-33.1	-33.1
Mn	-32.4	-32.4	-32.4
Fe	-31.7	-31.7	-31.7
Co	-31.6	-31.6	-31.6
Ni	-31.6	-31.6	-31.6
Cu	-24.9	-24.5	24.5
Zn	-31.2	-31.3	-31.3

Table S16: The effect of the plane wave energy cut off on the H<sub>2</sub>O binding energies (in kJ/mol) was tested for all of the M<sub>2</sub>(dobdc) with the opt88B-vdW functional. Aside from the single point calculation, a full geometry optimization was performed (no rigid framework approximation).

Metal	550 eV	SP with 1000 eV	1000 eV
Mg	-85.4	-86.0	-86.0
Mn	-69.4	-70.5	-70.5
Fe	-70.7	-71.7	-71.8
Co	-70.2	-70.1	-70.0
Ni	-80.9	-83.6	-83.5
Cu	-44.9	-44.0	-44.0
Zn	-63.6	-64.8	-64.8

Table S17: The calculated electronic binding energies were compared to experimental enthalpies. To make this comparison, the thermal energy and zero point energy were subtracted from the experimental values. These were taken to be equal to these values obtained at the vdW-DF2 level of theory by Lee et al. Energies in kJ/mol.

Guest	Mg	Mn	Fe	Co	Ni	Cu	Zn
CO <sub>2</sub>	3.7384	3.6178	3.6156	3.6300	3.6624	3.6178	3.6241
H <sub>2</sub> O	6.3642	5.9782	6.1491	6.2052	6.5686	4.3063	6.0446
CH <sub>4</sub>	4.7681	4.0328	4.3959	4.3782	4.3013	4.3614	4.5723

Table S18: The calculated thermal energy and zero point energy in kJ/mol for CO<sub>2</sub> in Mg<sub>2</sub>(dobdc) with the four vdW functionals.

Functional	Mg
optB88-vdW	3.721
optB86b-vdW	3.715
vdW-DF2	3.738
rev-vdW-DF2	3.724

## 4 Bond Energy Decomposition

In order to explore the differences between the nonlocal vdW functionals in more detail, we decomposed the contributions to the interaction energy for a single path where CO<sub>2</sub> is approaching the metal center in Mg<sub>2</sub>(dobdc). The interaction energy (E) can be decomposed into the exchange energy (E<sub>Ex</sub>), the local correlation energy (E<sub>LDA</sub>), the non-local vdW-correlation energy (E<sub>vdw</sub>), the Coulomb energy, and the kinetic energy (see Figure S1). As was shown for the binding energies at the minimum geometry, the optB88-vdW and optB86b-vdW functionals bind CO<sub>2</sub> significantly stronger than the vdW-DF2 and rev-vdW-DF2 functionals. The E<sub>LDA</sub> differs slightly between the four functionals likely due to the differences in the carbon-oxygen bond distance in CO<sub>2</sub> between these functionals. On the other hand, the vdW kernel employed in the optB88-vdW and optB86b-vdW functional differs from the one used in vdW-DF2 and rev-vdW-DF2. This difference is responsible for the different binding energetics observed for all of the guests. On the other hand, the optB88-vdW and optB86b-vdW functionals differ in which exchange functional is used; however, along the CO<sub>2</sub> approach path, this difference is relatively small. Likewise, the rev-vdW-DF2 and vdW-DF2 functionals differ in the exchange energy. The exchange term approaches large negative values at a larger distance from the metal center in the vdW-DF2 functional leading to the longer minimum M-O<sub>CO<sub>2</sub></sub> bond distance observed.

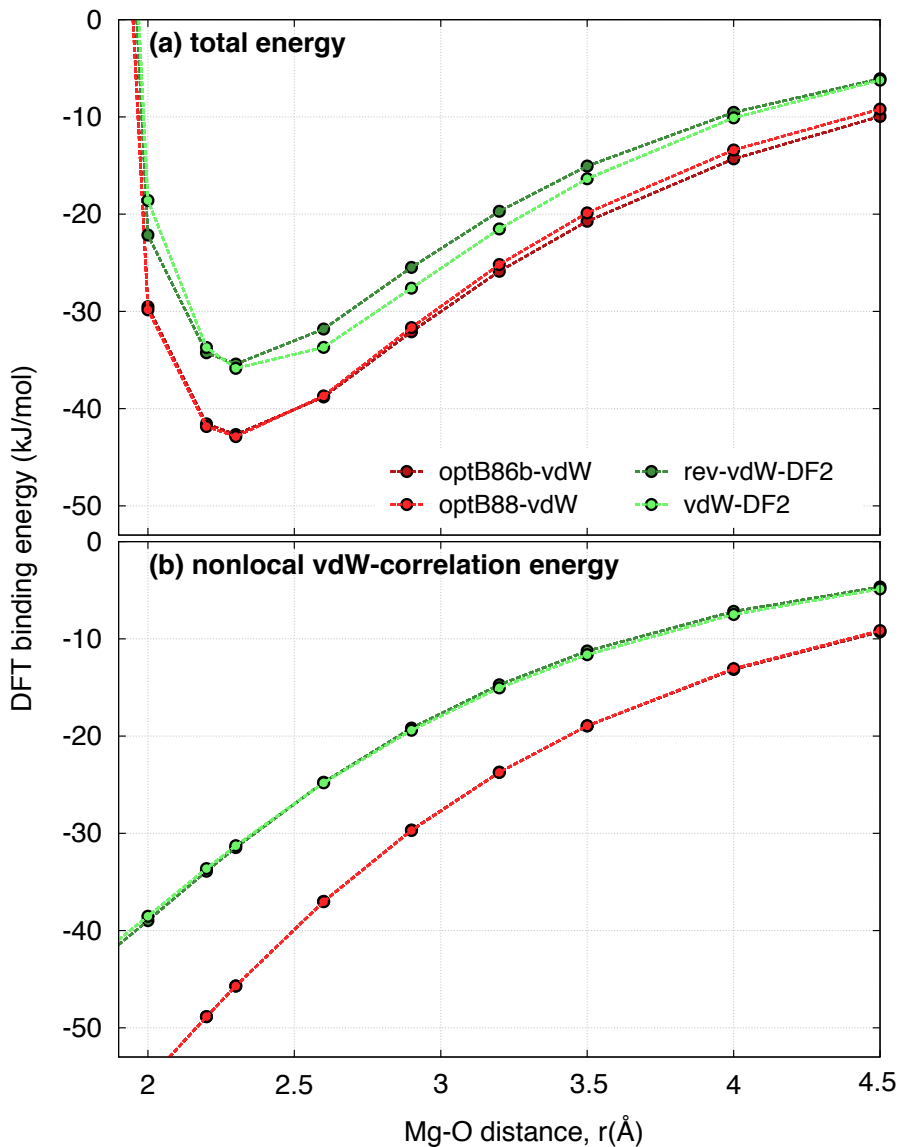


Figure S1: Comparison of the  $\text{CO}_2$ -framework interaction energies (kJ/mol) as a function of distance obtained with four DFT functionals. Figure shows total interaction energy (a) and (b) Nonlocal vdW-Correlation Energy.

Table S19: The CO<sub>2</sub>-framework interaction energies (kJ/mol) have been decomposed into three parts: Exchange Energy, Local Correlation Energy, and Nonlocal vdW-Correlation Energy. There values at the vdW-DF2 optimized geometry employing the rigid framework approximation are given.

Functional	Total Energy	Exchange Energy	Local Correlation Energy	Nonlocal vdW-Correlation Energy
optB88-vdW	-65.54	-15.54	-7.82	-52.49
optB86b-vdW	-65.71	-14.08	-7.89	-52.47
vdW-DF2	-37.78	-35.72	-8.24	-36.03
rev-vdW-DF2	-36.37	-21.33	-7.46	-36.32

## 5 Crystal structure details and Rietveld refinement plots

Table S20: Rietveld refinement results of Mg<sub>2</sub>(dobdc) loaded with 0.75 CD<sub>4</sub> : Mg, measured at 8 K.

Atom	X	Y	Z	Occupancy	Uiso (Å <sup>2</sup> )	Multiplicity
Mg1	0.3800(5)	0.3534(5)	0.135(2)	1	0.035(3)	18
O1	0.3226(4)	0.2945(4)	0.362(1)	1	0.021(3)	18
O2	0.3038(4)	0.2302(4)	0.594(1)	1	0.012(2)	18
O3	0.3559(4)	0.2730(5)	0.005(1)	1	0.024(3)	18
C1	0.3164(4)	0.2458(4)	0.419(1)	1	0.029(2)	18
C2	0.3274(4)	0.2054(3)	0.287(1)	1	0.019(2)	18
C3	0.3451(3)	0.2239(3)	0.085(1)	1	0.003(2)	18
C4	0.3530(3)	0.1846(4)	-0.0251(9)	1	0.008(2)	18
H1	0.3643(6)	0.1933(5)	-0.178(1)	1	0.015	18
C11	0.1974(3)	0.1855(3)	-0.0363(9)	0.745(5)	0.029(4)	18
D11	0.2245(5)	0.1724(5)	0.879(2)	0.745(5)	0.079(3)	18
D12	0.1794(5)	0.2064(5)	0.869(2)	0.745(5)	0.079(3)	18
D13	0.1609(4)	0.1461(4)	0.031(2)	0.745(5)	0.079(3)	18
D14	0.2247(5)	0.2167(4)	0.077(1)	0.745(5)	0.079(3)	18

Refined CD<sub>4</sub> : Mg = 0.745(5).

Goodness-of-fit parameters:  $\chi^2 = 1.721$ , Rp = 2.38%, wRp = 2.83%, wR<sub>exp</sub> = 2.18%.

Space group R-3;  $\lambda = 2.078 \text{ \AA}$ ; unit cell parameters: a = 25.9035(9) Å, c = 6.8836(3) Å, and V = 4000.0(3) Å<sup>3</sup>.

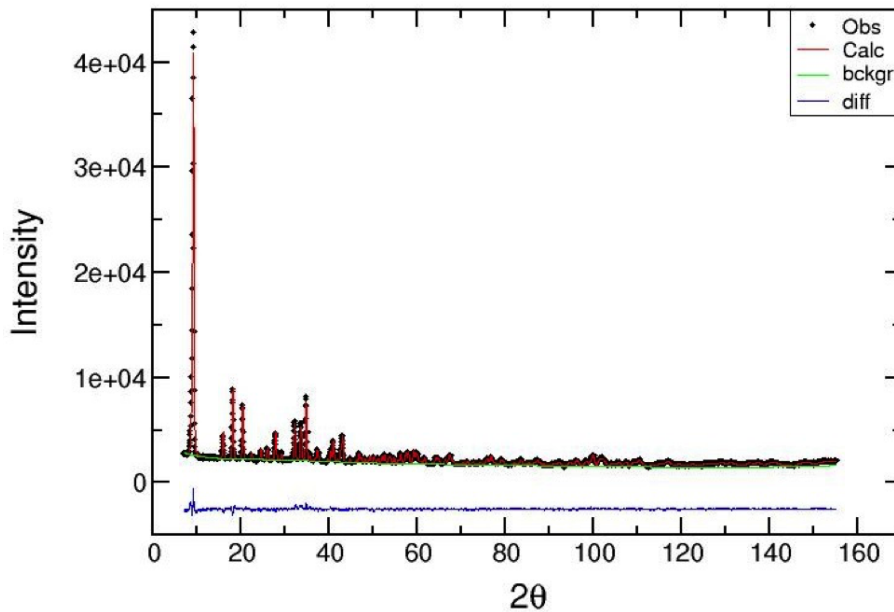


Figure S2: Rietveld refinement plot for  $\text{Mg}_2(\text{dobdc})$  loaded with 0.75  $\text{CD}_4 : \text{Mg}$ .

Table S21: Rietveld refinement results of  $\text{Mn}_2(\text{dobdc})$  loaded with 0.75  $\text{CD}_4 : \text{Mn}$ , measured at 8 K.

Atom	X	Y	Z	Occupancy	$U_{\text{iso}}$ ( $\text{\AA}^2$ )	Multiplicity
Mn1	0.3884(7)	0.356(1)	0.138(3)	1	0.001(6)	18
O1	0.3224(7)	0.2919(6)	0.354(2)	1	0.024(4)	18
O2	0.3010(6)	0.2304(6)	0.584(2)	1	0.009(3)	18
O3	0.3549(7)	0.2743(8)	0.007(3)	1	0.035(5)	18
C1	0.3167(6)	0.2450(6)	0.421(2)	1	0.030(4)	18
C2	0.3281(7)	0.2049(5)	0.303(2)	1	0.045(5)	18
C3	0.3437(8)	0.2238(6)	0.086(2)	1	0.034(4)	18
C4	0.3530(6)	0.1851(5)	-0.015(1)	1	0.022(4)	18
H1	0.364(1)	0.1938(9)	-0.165(2)	1	0.025	18
C11	0.1954(4)	0.1826(4)	-0.020(2)	0.556(6)	0.044(9)	18
D11	0.2261(8)	0.173(1)	0.908(3)	0.556(6)	0.055(4)	18
D12	0.1798(9)	0.2037(9)	0.882(3)	0.556(6)	0.055(4)	18
D13	0.1582(7)	0.1420(6)	0.033(3)	0.556(6)	0.055(4)	18
D14	0.2175(9)	0.2120(8)	0.099(2)	0.556(6)	0.055(4)	18

Refined  $\text{CD}_4 : \text{Mn} = 0.556(6)$ .

Goodness-of-fit parameters:  $\chi^2 = 2.256$ ,  $R_p = 2.43\%$ ,  $wR_p = 2.98\%$ ,  $wR_{exp} = 2.00\%$ .

Space group R-3;  $\lambda = 2.078 \text{ \AA}$ ; unit cell parameters:  $a = 26.295(1) \text{ \AA}$ ,  $c = 7.0724(5) \text{ \AA}$ , and  $V = 4234.8(5) \text{ \AA}^3$ .

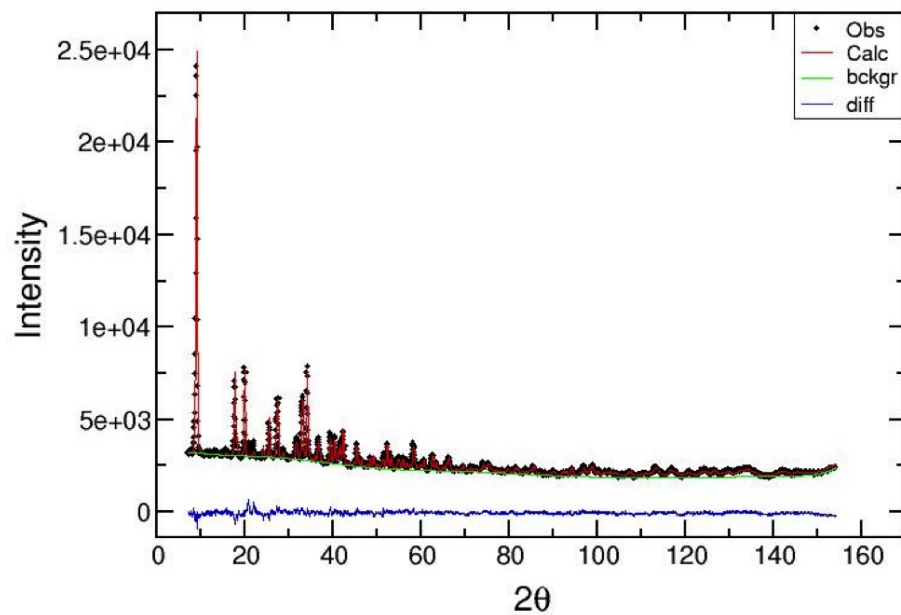


Figure S3: Rietveld refinement plot for  $\text{Mn}_2(\text{dobdc})$  loaded with 0.75  $\text{CD}_4 : \text{Mn}$ .

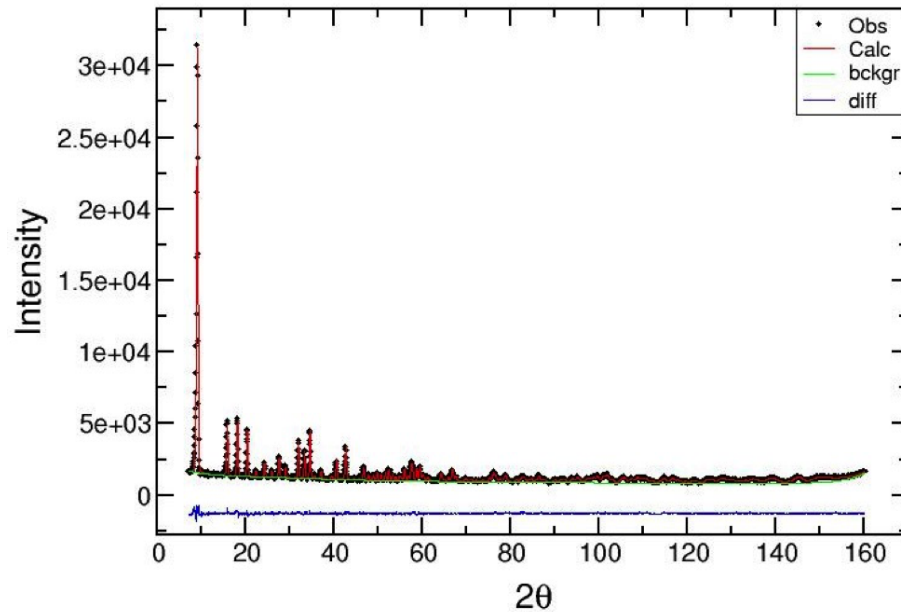


Figure S4: Rietveld refinement plot for  $\text{Fe}_2(\text{dobdc})$  loaded with 0.75  $\text{CD}_4 : \text{Fe}$ .

Table S22: Rietveld refinement results of  $\text{Fe}_2(\text{dobdc})$  loaded with 0.75  $\text{CD}_4 : \text{Fe}$ , measured at 8 K.

Atom	X	Y	Z	Occupancy	$U_{\text{iso}} (\text{\AA}^2)$	Multiplicity
Fe1	0.3818(2)	0.3513(2)	0.1416(7)	1	0.010(1)	18
O1	0.3251(4)	0.2957(4)	0.3582(1)	1	0.020(2)	18
O2	0.3005(4)	0.2273(4)	0.594(1)	1	0.024(3)	18
O3	0.3525(4)	0.2742(4)	0.006(1)	1	0.008(2)	18
C1	0.3165(4)	0.2447(4)	0.420(1)	1	0.015(2)	18
C2	0.3262(4)	0.2056(3)	0.289(1)	1	0.009(2)	18
C3	0.3423(4)	0.2216(3)	0.087(1)	1	0.006(2)	18
C4	0.3497(4)	0.1809(4)	-0.0273(9)	1	0.009(2)	18
H1	0.3619(7)	0.1913(6)	-0.180(1)	1	0.025	18
C11	0.1975(8)	0.1861(9)	-0.025(2)	0.678(6)	0.064(6)	18
D11	0.2232(8)	0.1730(7)	0.894(3)	0.678(6)	0.113(5)	18
D12	0.1795(7)	0.2083(7)	0.884(3)	0.678(6)	0.113(5)	18
D13	0.1583(7)	0.1462(7)	0.041(3)	0.678(6)	0.113(5)	18
D14	0.2215(9)	0.2148(9)	0.098(2)	0.678(6)	0.113(5)	18

Refined  $\text{CD}_4 : \text{Fe} = 0.678(6)$ .

Goodness-of-fit parameters:  $\chi^2 = 1.330$ ,  $R_p = 2.61\%$ ,  $wR_p = 3.23\%$ ,  $wR_{exp} = 2.82\%$ .

Space group R-3;  $\lambda = 2.078 \text{ \AA}$ ; unit cell paramters:  $a = 26.1159(7) \text{ \AA}$ ,  $c = 6.8716(3) \text{ \AA}$ , and  $V = 4058.8(2) \text{ \AA}^3$ .

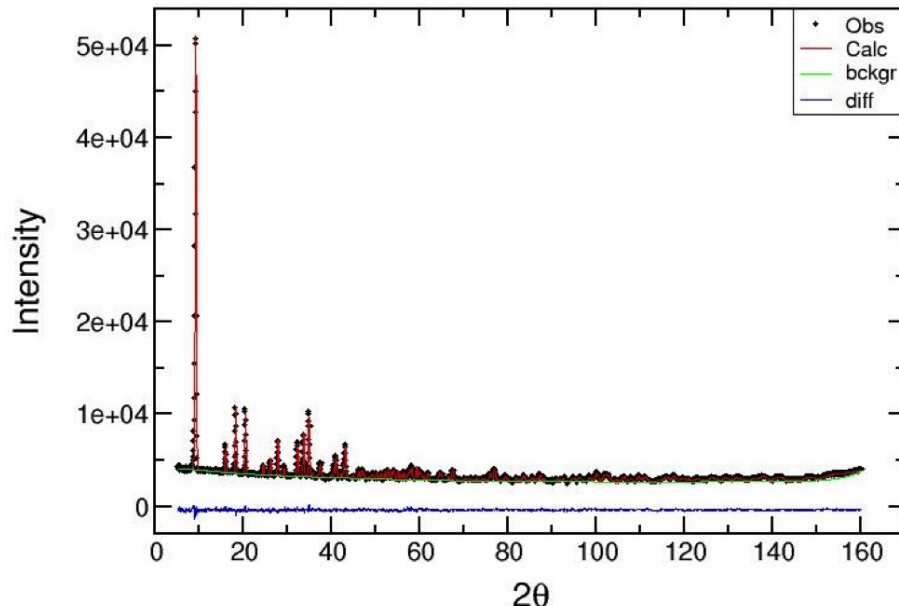


Figure S5: Rietveld refinement plot for  $\text{Co}_2(\text{dobdc})$  loaded with 0.75  $\text{CD}_4 : \text{Co}$ .

Table S23: Rietveld refinement results of  $\text{Co}_2(\text{dobdc})$  loaded with 0.75  $\text{CD}_4 : \text{Co}$ , measured at 8 K.

Atom	X	Y	Z	Occupancy	$U_{\text{iso}} (\text{\AA}^2)$	Multiplicity
Co1	0.3817(9)	0.3519(9)	0.132(2)	1	0.004(5)	18
O1	0.3256(4)	0.2974(4)	0.374(2)	1	0.029(3)	18
O2	0.3015(4)	0.2267(3)	0.602(1)	1	0.002(2)	18
O3	0.3543(4)	0.2736(4)	0.006(1)	1	0.003(2)	18
C1	0.3141(4)	0.2472(4)	0.426(1)	1	0.040(3)	18
C2	0.3273(4)	0.2070(4)	0.287(1)	1	0.022(2)	18
C3	0.3474(4)	0.2248(4)	0.089(1)	1	0.026(2)	18
C4	0.3526(4)	0.1831(4)	-0.0287(9)	1	0.016(2)	18
H1	0.3643(7)	0.1927(6)	-0.182(1)	1	0.028(4)	18
C11	0.1954(3)	0.1859(3)	-0.023(1)	0.627(5)	0.053(5)	18
D11	0.2224(8)	0.1799(7)	0.868(3)	0.627(5)	0.127(6)	18
D12	0.1663(7)	0.1992(9)	0.906(3)	0.627(5)	0.127(6)	18
D13	0.1684(7)	0.1441(4)	0.055(2)	0.627(5)	0.127(6)	18
D14	0.2242(7)	0.2203(6)	0.081(2)	0.627(5)	0.127(6)	18

Refined  $\text{CD}_4 : \text{Co} = 0.627(5)$ .

Goodness-of-fit parameters:  $\chi^2 = 1.596$ ,  $R_p = 1.78\%$ ,  $wR_p = 2.17\%$ ,  $wR_{exp} = 1.73\%$ .

Space group R-3;  $\lambda = 2.078 \text{ \AA}$ ; unit cell parameters:  $a = 25.8840(7) \text{ \AA}$ ,  $c = 6.8551(3) \text{ \AA}$  and  $V = 3977.4(2) \text{ \AA}^3$ .

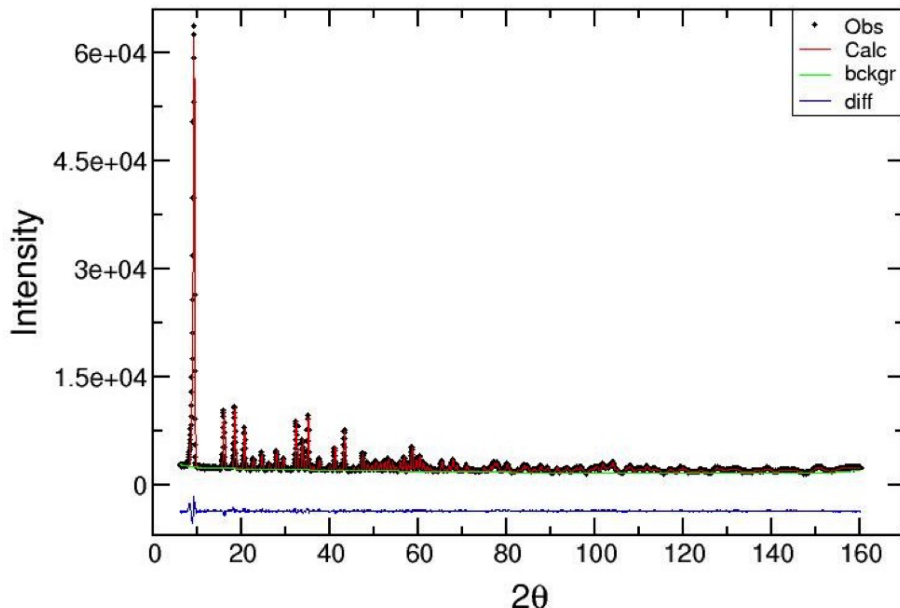


Figure S6: Rietveld refinement plot for  $\text{Ni}_2(\text{dobdc})$  loaded with 0.75  $\text{CD}_4 : \text{Ni}$ .

Table S24: Rietveld refinement results of Ni<sub>2</sub>(dobdc) loaded with 0.75 CD<sub>4</sub> : Ni, measured at 8 K.

Atom	X	Y	Z	Occupancy	Uiso (Å <sup>2</sup> )	Multiplicity
Ni1	0.3813(2)	0.3507(2)	0.1424(6)	1	0.020(1)	18
O1	0.3259(3)	0.2966(3)	0.365(1)	1	0.013(2)	18
O2	0.3025(4)	0.2294(4)	0.605(1)	1	0.024(2)	18
O3	0.3556(4)	0.2757(4)	0.004(1)	1	0.017(2)	18
C1	0.3187(3)	0.2474(3)	0.423(1)	1	0.015(2)	18
C2	0.3277(3)	0.2066(3)	0.293(1)	1	0.024(2)	18
C3	0.3440(4)	0.2220(3)	0.086(1)	1	0.032(2)	18
C4	0.3514(4)	0.1831(4)	-0.033(1)	1	0.030(2)	18
H4	0.3650(6)	0.1925(6)	-0.169(2)	1	0.022(3)	18
C11	0.1940(3)	0.1828(3)	-0.0258(7)	0.692(4)	0.025(3)	18
D11	0.2217(4)	0.1765(4)	0.866(1)	0.692(4)	0.064(3)	18
D12	0.1676(4)	0.1994(4)	0.900(2)	0.692(4)	0.064(3)	18
D13	0.1640(4)	0.1402(3)	0.046(1)	0.692(4)	0.064(3)	18
D14	0.2226(5)	0.2153(4)	0.085(1)	0.692(4)	0.064(3)	32

Refined CD<sub>4</sub> : Ni = 0.692(4).

Goodness-of-fit parameters:  $\chi^2 = 2.280$ , Rp = 2.49%, wRp = 3.04%, wR<sub>exp</sub> = 2.03%.

Space group R-3;  $\lambda$  = 2.078 Å; unit cell parameters: a = 25.7869(6) Å, c = 6.7571(2) Å, and V = 3891.3(2) Å<sup>3</sup>.

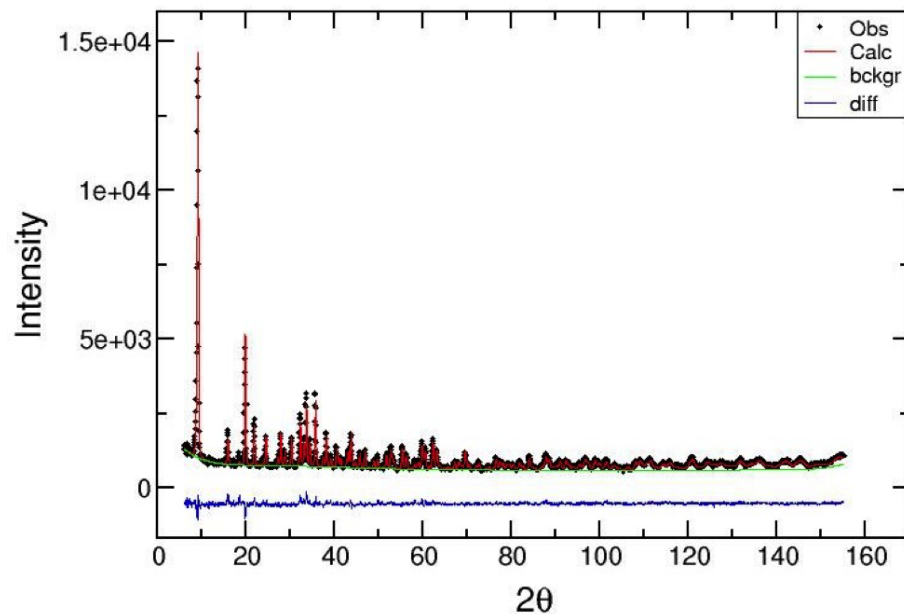


Figure S7: Rietveld refinement plot for Cu<sub>2</sub>(dobdc) loaded with 0.75 CD<sub>4</sub> : Cu.

Table S25: Rietveld refinement results of Cu<sub>2</sub>(dobdc) loaded with 0.75 CD<sub>4</sub> : Cu, measured at 8 K.

Atom	X	Y	Z	Occupancy	Uiso (Å <sup>2</sup> )	Multiplicity
Cu1	0.3875(3)	0.3494(4)	0.176(1)	1	0.003(2)	18
O1	0.3532(5)	0.3037(5)	0.439(2)	1	0.001(2)	18
O2	0.2925(5)	0.2250(4)	0.629(2)	1	0.001(2)	18
O3	0.3608(5)	0.2783(5)	0.002(2)	1	0.001(2)	18
C1	0.3234(4)	0.2477(4)	0.466(2)	1	0.008(1)	18
C2	0.3277(4)	0.2059(4)	0.307(2)	1	0.008(1)	18
C3	0.3483(5)	0.2251(4)	0.099(2)	1	0.008(1)	18
C4	0.3538(4)	0.1836(5)	-0.040(1)	1	0.008(1)	18
H	0.3686(8)	0.1934(8)	-0.196(2)	1	0.023(5)	18
C11	0.1785(3)	0.1590(3)	0.029(1)	0.823(6)	0.041(5)	18
D11	0.2142(5)	0.1525(6)	0.966(3)	0.823(6)	0.080(4)	18
D12	0.1674(7)	0.1831(6)	0.911(2)	0.823(6)	0.080(4)	18
D13	0.1393(4)	0.1156(4)	0.060(3)	0.823(6)	0.080(4)	18
D14	0.1930(6)	0.1846(6)	0.177(2)	0.823(6)	0.080(4)	18

Refined CD<sub>4</sub> : Cu = 0.823(6).

Goodness-of-fit parameters:  $\chi^2 = 1.724$ , Rp = 3.75%, wRp = 4.43%, wR<sub>exp</sub> = 3.41%.

Space group R-3;  $\lambda = 2.078 \text{ \AA}$ ; unit cell parameters: a = 25.8666(9) Å, c = 6.2513(3) Å, and V = 3622.2(3) Å<sup>3</sup>.

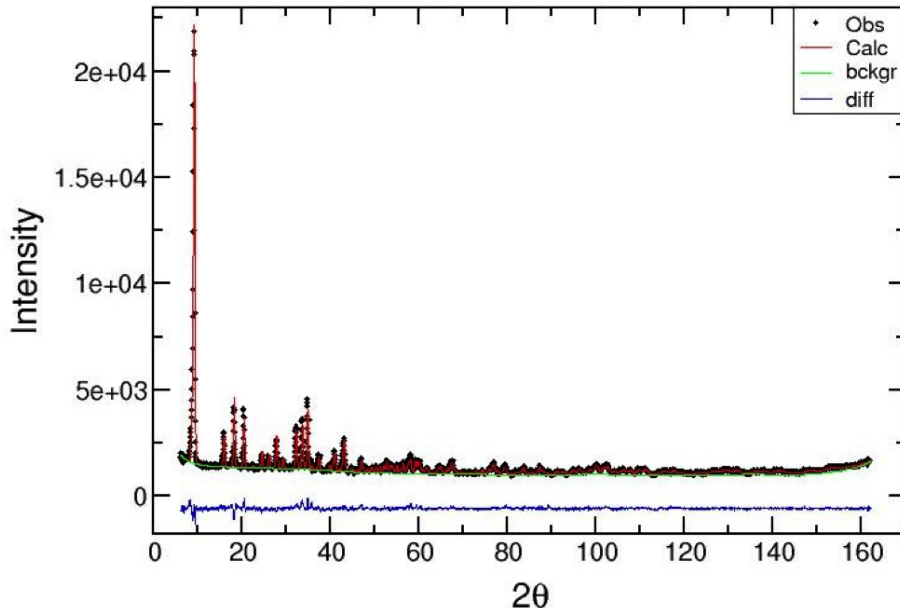


Figure S8: Rietveld refinement plot for Zn<sub>2</sub>(dobdc) loaded with 0.75 CD<sub>4</sub> : Zn.

Table S26: Rietveld refinement results of  $\text{Zn}_2(\text{dobdc})$  loaded with 0.75  $\text{CD}_4 : \text{Zn}$ , measured at 8 K.

Atom	X	Y	Z	Occupancy	$\text{U}_{\text{iso}} (\text{\AA}^2)$	Multiplicity
Zn1	0.3823(6)	0.3527(6)	0.131(2)	1	0.012(3)	18
O1	0.3226(5)	0.2917(5)	0.359(2)	1	0.010(3)	18
O2	0.3037(6)	0.2269(5)	0.610(1)	1	0.013(3)	18
O3	0.3524(6)	0.2712(7)	0.008(2)	1	0.033(4)	18
C1	0.3147(6)	0.2435(4)	0.430(1)	1	0.024(3)	18
C2	0.3262(6)	0.2070(4)	0.288(1)	1	0.038(4)	18
C3	0.3459(6)	0.2239(5)	0.093(1)	1	0.033(4)	18
C4	0.3530(6)	0.1829(4)	-0.024(2)	1	0.025(4)	18
H1	0.3636(9)	0.1952(8)	-0.177(2)	1	0.025	18
C11	0.1898(5)	0.1787(4)	-0.026(1)	0.629(6)	0.018(6)	18
D11	0.2134(8)	0.1621(8)	0.886(3)	0.629(6)	0.066(5)	18
D12	0.1712(8)	0.1992(8)	0.880(3)	0.629(6)	0.066(5)	18
D13	0.1542(7)	0.1422(6)	0.055(2)	0.629(6)	0.066(5)	18
D14	0.2207(7)	0.2118(7)	0.077(2)	0.629(6)	0.066(5)	18

Refined  $\text{CD}_4 : \text{Zn} = 0.629(6)$ .

Goodness-of-fit parameters:  $\chi^2 = 1.729$ ,  $\text{Rp} = 2.95\%$ ,  $\text{wRp} = 3.59\%$ ,  $\text{wR}_{\text{exp}} = 2.76\%$ .

Space group R-3;  $\lambda = 2.078 \text{ \AA}$ ; unit cell parameters:  $a = 25.884(1) \text{ \AA}$ ,  $c = 6.8520(5) \text{ \AA}$ , and  $V = 3975.7(4) \text{ \AA}^3$ .